

# An adjustable oxide-free tunnel junction for vibrational spectroscopy of molecules

Darin T. Zimmerman<sup>a)</sup>

*Department of Physics, Penn State Altoona College, Altoona, Pennsylvania 16601-3760*

Michael B. Weimer and Glenn Agnolet

*Department of Physics, Texas A&M University, College Station, Texas 77843-4242*

(Received 14 June 1999; accepted for publication 23 August 1999)

We describe an adjustable, oxide-free, tunnel junction with the stability necessary to observe the vibrational modes of molecules adsorbed on clean metal surfaces. We illustrate the capabilities of this device with inelastic tunneling data from junctions whose barriers are formed by neon/acetylene mixtures of varying concentration. From the concentration dependence of the inelastic spectra, we can distinguish between acetylene molecules chemisorbed on the metal electrodes and those that are either physisorbed or incorporated in the neon barrier. © 1999 American Institute of Physics.

[S0003-6951(99)04542-8]

Since its inception in 1966,<sup>1</sup> inelastic electron tunneling spectroscopy (IETS) has been successfully applied to problems in surface chemistry, catalysis, and molecular vibrational spectroscopy.<sup>2-4</sup> In conventional IETS, the vibrational modes of molecules are detected by electrons that tunnel through the insulating barrier of a metal-oxide-metal junction. The molecules of interest are either deposited at the metal-oxide interface or incorporated within the oxide barrier. The versatility of tunneling spectroscopy would be significantly enhanced if an adjustable, oxide-free tunnel junction were available that enabled one to study molecules adsorbed on clean metal surfaces under ultra-high-vacuum conditions. Numerous unsuccessful attempts have been made to perform IETS in tunneling geometries that do not rely on an oxide barrier. These include squeezable tunnel junctions<sup>5</sup> and mechanically controlled break junctions.<sup>6</sup> Only recently<sup>7</sup> has inelastic tunneling spectroscopy been demonstrated in a scanning tunneling microscope (STM) geometry.<sup>8</sup>

We describe a geometry for inelastic tunneling spectroscopy, based on the self-assembling tunnel junction (SATJ) devised by Gregory,<sup>9,10</sup> in which the oxide barrier is replaced by an inert gas film. The SATJ is formed at the contact point<sup>11</sup> between two long, fine metallic wires ( $\sim 12 \mu\text{m}$  diam) mounted in a cross geometry<sup>12</sup> (Fig. 1, inset). One wire is parallel to an external magnetic field ( $\leq 0.5$  T) whereas the other has a curved section perpendicular to this field. The spacing between wires is adjusted by deflecting the curved one with the Lorentz force generated by a small dc current ( $< 10$  mA).

The wires are initially separated from each other and cleaned by resistive heating to 950 K for 1 h. Any contaminants evaporate from the wire surfaces and adhere to the walls of the cryostat which are maintained at 4.2 K. Heating also removes surface irregularities and leaves the wires relatively smooth as judged by scanning electron microscopy.

Once the wire surfaces have been cleaned, a tunnel barrier is deposited when gas of a predetermined composition is

admitted into the vacuum chamber and condenses on all cold surfaces. A junction is subsequently formed by bringing the wires together. Although the properties of any particular junction will depend on the composition and homogeneity of the adsorbed film, we are able to obtain stable junctions whose resistance ( $R_j$ ) ranges from 50 k $\Omega$  to 500 M $\Omega$  by varying the applied force. This adjustability is illustrated with a platinum/neon junction in Fig. 1. As the force applied to the junction is increased, the junction conductance quickly relaxes ( $\tau \sim 20$  s) to a value that reflects the controlled decrease in the barrier thickness.

The tunneling data presented here were obtained by sweeping the bias voltage ( $V$ ) between  $\pm 500$  mV in 1 h (17 mV/min). As in conventional IETS, the dc tunnel current ( $I$ ) and its first two derivatives were simultaneously measured using a standard ac modulation technique<sup>4</sup> in which the dc bias was modulated at 555 Hz with an amplitude of 15 mV<sub>rms</sub>. The second derivative signal  $d^2I/dV^2$  was then

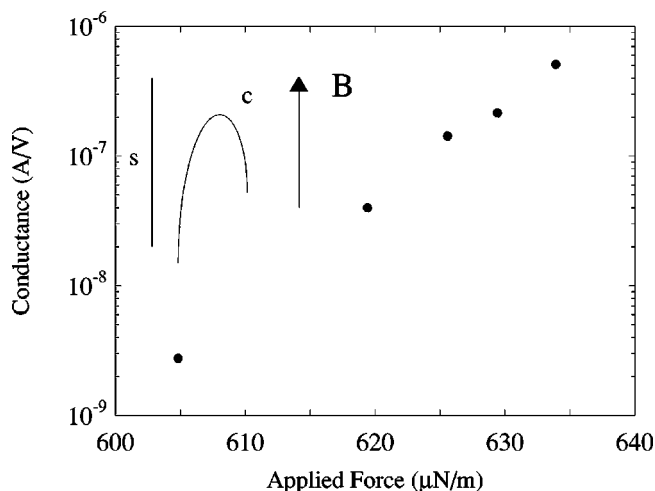


FIG. 1. Semilogarithmic plot illustrating the orders of magnitude adjustability in the dc conductance of a platinum/neon SATJ with applied force. The wire junction geometry is illustrated in the inset. The force, which controls the electrode separation, is varied by passing a small dc current through the curved wire (c) perpendicular to the external magnetic field (B). Data were taken with fixed bias voltage (0.3 V) at 4.2 K.

<sup>a)</sup>Electronic mail: dtz1@psu.edu

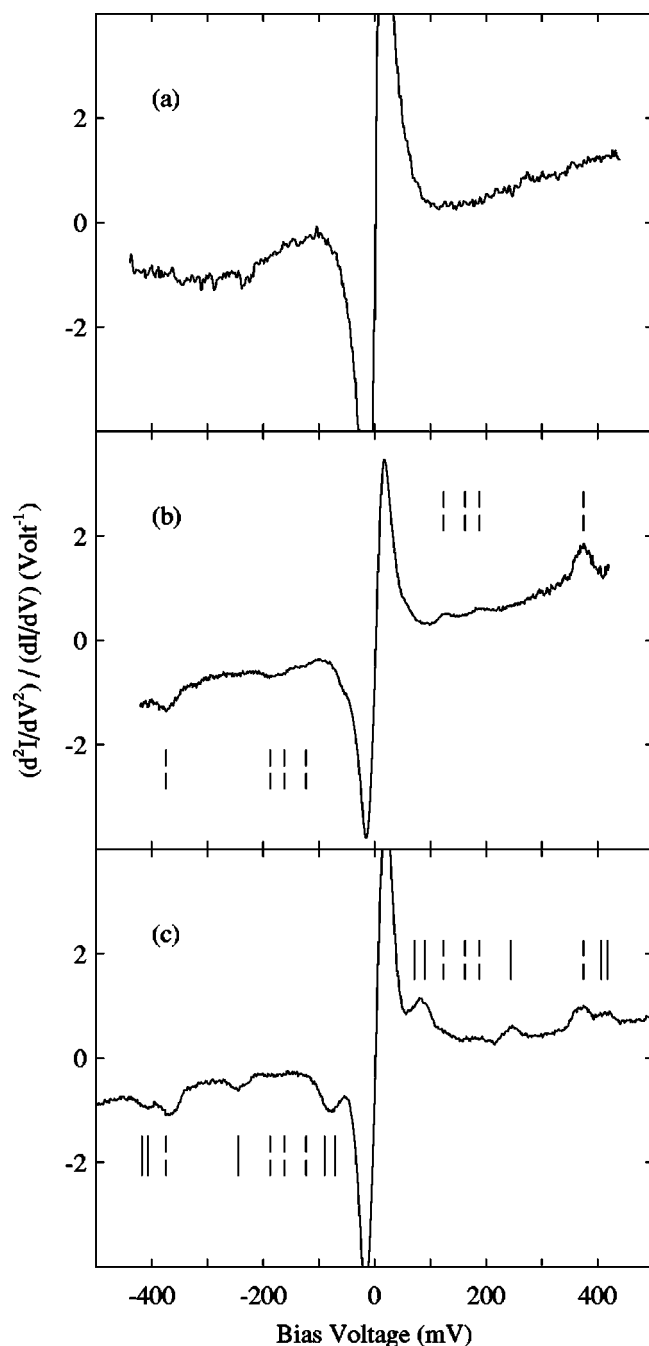


FIG. 2. Single-sweep IETS data of platinum wire junctions formed with (a) ultrapure neon ( $R_j=19\text{ M}\Omega$ ), (b) 5%  $\text{C}_2\text{H}_2/95\%$  Ne ( $R_j=1.4\text{ M}\Omega$ ), and (c) 25%  $\text{C}_2\text{H}_2/75\%$  Ne ( $R_j=24\text{ M}\Omega$ ). Dashed and solid vertical lines indicate surface and gas-phase vibrational modes, respectively.

scaled to the conductance ( $\sigma=dI/dV$ ) so that data from different junctions could be directly compared.<sup>13</sup>

Figure 2 shows the IETS data from three platinum wire junctions with barrier films consisting of (a) ultrapure neon (99.9995%), (b) neon with 5% acetylene,<sup>14</sup> and (c) neon with 25% acetylene. Each curve represents a single sweep of the bias voltage with no additional averaging beyond the lock-in amplifier time constant ( $\tau\sim 3\text{ s}$ ). The remaining noise is such that the threshold for detecting a change in the integrated intensity of individual inelastic peaks is  $\Delta\sigma/\sigma\sim 0.02\%$ , which suffices to resolve vibrational spectra.<sup>15</sup>

In common with Gregory,<sup>9,10</sup> all of our SATJs exhibit a pronounced zero-bias feature (ZBF) irrespective of the bar-

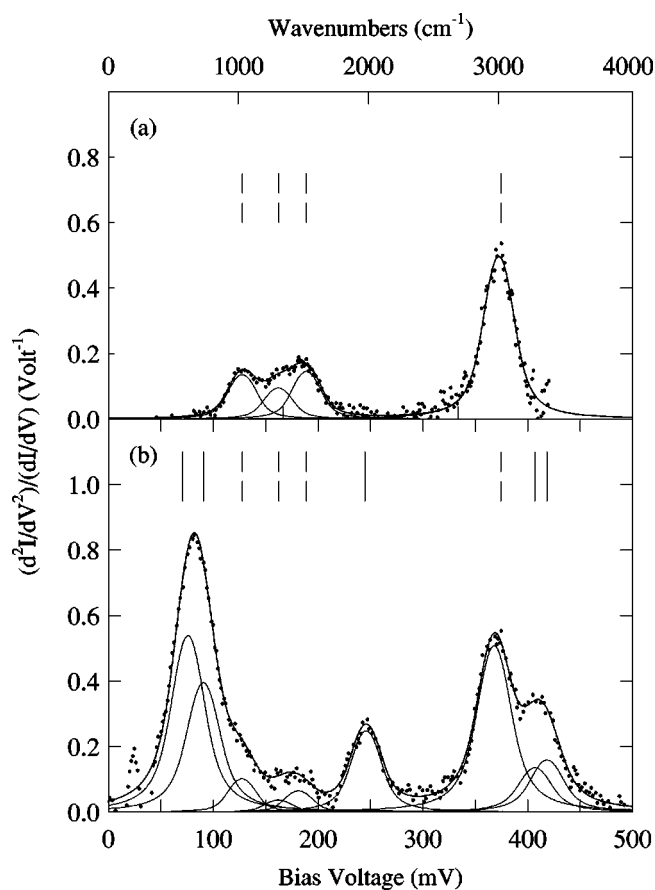


FIG. 3. Data from the doped junctions of Fig. 2 with background removed (solid symbols), together with the decomposition into individual IETS peaks (thin solid lines). The combined fit (heavy solid line) is also shown. Dashed and solid vertical lines indicate the surface vibrational modes observed with a 5%  $\text{C}_2\text{H}_2/95\%$  Ne mixture (a) and the additional gas-phase modes that appear in the enriched 25%  $\text{C}_2\text{H}_2/75\%$  Ne mixture (b), respectively.

rier gas or electrode composition. This ZBF represents a significant suppression of the junction conductance ( $\Delta\sigma/\sigma\sim 20\%$ ) within 50 meV of zero bias.<sup>16</sup> Similar ZBFs are observed in series junctions<sup>17</sup> and in current-biased junctions<sup>18</sup> where they are attributed to Coulomb blockade. ZBFs have also been attributed to nonequilibrium electron tunneling,<sup>19</sup> Kondo scattering,<sup>20</sup> and a suppression of the local density of states by adsorbates.<sup>21</sup>

The scaled second derivative signal from an ultrapure neon junction is shown in Fig. 2(a). Aside from the ever-present ZBF, the data exhibit no discernible structure. Junctions made with *doped* neon films [Figs. 2(b) and 2(c)], on the other hand, display prominent peaks outside the ZBF region that, as we shall see, are consistent with the known vibrational modes of  $\text{C}_2\text{H}_2$ . These inelastic peaks are symmetric in the bias voltage and reproducible over several days.

To analyze the data, we employ a theoretical fitting function that includes three distinct components: (i) a cubic function of the bias voltage to model the slowly varying background; (ii) Lorentzians convolved with a modulation measurement function<sup>22</sup> to fit the inelastic peaks; and (iii) the derivative of a convolved Lorentzian centered about zero-bias voltage to model the ZBF. The second derivative signals from the acetylene-doped junctions [Figs. 2(b) and 2(c)] are replotted in Fig. 3 with the cubic background and ZBF removed.

At low concentrations [5% C<sub>2</sub>H<sub>2</sub>/95% Ne; Figs. 2(b) and 3(a)], we observe an isolated peak at 372 meV that is consistent with the C–H stretching mode of C<sub>2</sub>H<sub>2</sub> on Pt (111) as measured by electron energy-loss spectroscopy.<sup>23,24</sup> Stipe, Rezaei, and Ho<sup>7</sup> also observe this mode in their STM measurement of C<sub>2</sub>H<sub>2</sub> on Cu (100). We, however, observe additional inelastic signals at lower energies (100–200 meV) in a range consistent with other C–H modes.<sup>25</sup> Although we cannot resolve individual modes in this region due to the large modulation employed in these datasets, it is clear that the sharp boundaries at the extremes of this region define two inelastic peaks. The lower peak (128 meV) appears close to the C–H bending mode of C<sub>2</sub>H<sub>2</sub> on Pt (123 meV).<sup>23,24</sup> The upper peak (189 meV) is not associated with a known C<sub>2</sub>H<sub>2</sub> vibrational mode but its energy is similar to the C–C modes found in related organometallic complexes.<sup>24</sup> If we restrict the widths of the 128 and 189 meV peaks to be comparable to that of the 372 meV peak, the data are consistent with a third peak at 160 meV, which corresponds to the C–C stretching mode of C<sub>2</sub>H<sub>2</sub> on Pt.<sup>23,24</sup> As with the 372 meV C–H stretch, these lower-energy modes are present in all of our doped junctions.

With the addition of further acetylene, [25% C<sub>2</sub>H<sub>2</sub>/75% Ne; Figs. 2(c) and 3(b)], there is little change in the intensities or positions of the peaks observed at the lower concentration. We see instead the emergence of five *new* peaks. As indicated in Fig. 3(b), these additional peaks are well fit by a complete set of vibrational modes of C<sub>2</sub>H<sub>2</sub> in the gas phase (both infrared and Raman active) at their accepted energies (76, 91, 245, 407, and 418 meV).<sup>26</sup> This observation suggests that the 5% data already correspond to a saturated monolayer of chemisorbed molecules; additional C<sub>2</sub>H<sub>2</sub> must then be either physisorbed or incorporated into the Ne matrix, consistent with the emergence of “gas-like” peaks at higher concentrations.

Finally, it is worth noting that if the surface coverage in these experiments is, as we believe, a saturated monolayer, then the integrated intensity of the 372 meV mode ( $\Delta\sigma/\sigma \sim 0.026$ ) is an order of magnitude larger than expected on the basis of conventional dipole scattering.<sup>27</sup> A similar enhancement of  $\Delta\sigma/\sigma$  was observed by Stipe, Rezaei, and Ho.<sup>7</sup>

To summarize, we have described an adjustable, oxide-free tunnel junction for inelastic electron tunneling spectroscopy based on the SATJ design. We have demonstrated the device has the stability necessary to perform vibrational spectroscopy of molecules adsorbed on clean metal surfaces and that the second derivative signal from inert barrier films (neon) is relatively featureless over the energy range of interest. In spite of the large modulation voltage used in these initial experiments, we can clearly distinguish between molecules chemisorbed on the metal electrodes and those that are either physisorbed or incorporated in the neon barrier. Given our existing signal to noise, an energy resolution com-

parable to that obtained with other spectroscopic techniques<sup>28</sup> should be easily achieved by reducing the ac modulation to 1–2 meV and signal averaging over multiple sweeps of the bias voltage.

This work was supported by the National Science Foundation, the Texas Advanced Research Program, and the Robert A. Welch Foundation.

<sup>1</sup>R. C. Jaklevic and J. Lambe, Phys. Rev. Lett. **17**, 1139 (1966).

<sup>2</sup>K. W. Hipps and U. Mazur, J. Phys. Chem. **97**, 7803 (1993), and references therein.

<sup>3</sup>P. K. Hansma, *Tunneling Spectroscopy: Capabilities, Applications, and New Techniques* (Plenum, New York, 1982), and articles therein.

<sup>4</sup>P. K. Hansma, Phys. Rep. **30C**, 145 (1977).

<sup>5</sup>J. Moreland, S. Alexander, M. Cox, R. Sonnenfeld, and P. K. Hansma, Appl. Phys. Lett. **43**, 387 (1983).

<sup>6</sup>J. Moreland and J. W. Ekin, J. Appl. Phys. **58**, 3888 (1985).

<sup>7</sup>The inelastic vibrational spectrum of a single molecule of C<sub>2</sub>H<sub>2</sub> has been observed with a low-temperature STM [B. C. Stipe, M. A. Rezaei, and W. Ho, Science **280**, 1732 (1998); Phys. Rev. Lett. **82**, 1724 (1999)].

<sup>8</sup>G. Binnig, N. Garcia, and H. Rohrer, Phys. Rev. B **32**, 1336 (1985).

<sup>9</sup>S. Gregory, Phys. Rev. Lett. **64**, 689 (1990).

<sup>10</sup>S. Gregory, Phys. Rev. B **44**, 12868 (1991).

<sup>11</sup>The results presented here do not depend upon the junction area, which has not yet been satisfactorily characterized. However, very crude estimates of this area, based on a comparison of the actual junction conductance with a semiclassical approximation to the conductance density [W. F. Brinkman, R. C. Dynes, and J. M. Rowell, J. Appl. Phys. **41**, 1915 (1970)], yield an upper limit of 1000 nm<sup>2</sup>. This limit implies there are fewer than 10<sup>4</sup> molecules, per adsorbed monolayer, within a typical junction.

<sup>12</sup>D. T. Zimmerman, M. B. Weimer, and G. Agnolet, Czech. J. Phys. **46**, 2835 (1996).

<sup>13</sup>With this scaling, the intensity of a vibrational mode  $\Delta\sigma/\sigma$  is equal to the integrated peak area.

<sup>14</sup>Acetylene of unknown purity was mixed with the neon carrier gas at room temperature and then filtered through a liquid-nitrogen trap before adsorption; quoted concentrations refer to the room-temperature mixture.

<sup>15</sup>P. K. Hansma, IBM J. Res. Dev. **30**, 370 (1986).

<sup>16</sup>For pure Ne barriers,  $\Delta\sigma/\sigma$  decreases as the conductance of the junction increases. Gregory also observed this trend and attributed it to the coupling of tunneling electrons to the electromagnetic environment in large conductance junctions (see Ref. 10).

<sup>17</sup>R. Wilkins, E. Ben-Jacob, and R. C. Jaklevic, Phys. Rev. Lett. **63**, 801 (1989).

<sup>18</sup>D. V. Averin and K. K. Likharev, J. Low Temp. Phys. **62**, 345 (1986).

<sup>19</sup>P. N. Trofimenkoff, H. J. Kreuzer, W. J. Wattamaniuk, and J. G. Adler, Phys. Rev. Lett. **29**, 597 (1972).

<sup>20</sup>D. C. Ralph and R. A. Buhrman, Phys. Rev. Lett. **69**, 2118 (1992).

<sup>21</sup>R. J. P. Keijsers, J. Voets, O. I. Shklyarevskii, and H. van Kempen, Phys. Rev. Lett. **76**, 1138 (1996).

<sup>22</sup>J. Klein, A. Léger, M. Belin, D. Défourneau, and M. J. L. Sangster, Phys. Rev. B **7**, 2336 (1973).

<sup>23</sup>H. Ibach and S. Lehwald, J. Vac. Sci. Technol. **15**, 407 (1978).

<sup>24</sup>N. R. Avery, Langmuir **4**, 445 (1988).

<sup>25</sup>F. P. Netzer and M. G. Ramsey, Crit. Rev. Solid State Mater. Sci. **17**, 397 (1992).

<sup>26</sup>T. Shimanouchi, *Tables of Molecular Vibrational Frequencies*, (National Bureau of Standards, 1972), consolidated Vol. I.

<sup>27</sup>D. J. Scalapino and S. M. Marcus, Phys. Rev. Lett. **18**, 459 (1967).

<sup>28</sup>L. H. Dubois, in *Tunneling Spectroscopy: Capabilities, Applications and New Techniques*, edited by P. K. Hansma (Plenum, New York, 1982), p. 153.